

region in the  $\pi\eta$  final state both for events in which the  $\eta$  decays into neutrals and into charged particles. However, the question of a  $K\bar{K}$  decay mode is still somewhat open experimentally, it being not clearly established that the  $K\bar{K}$  enhancement near threshold, the  $\pi_N(1016)$ ,<sup>4</sup> represents an alternative decay mode of this object, as has been suggested.<sup>5</sup>

The widths of the reported enhancements are likewise somewhat of a puzzle and range from a value  $< 5$  MeV using the missing-mass spectrometer<sup>2</sup> up to our own value of  $80 \pm 30$  MeV. It is difficult to reconcile these widths. On the other hand, it is not certain that

the  $\delta(962)$  represents the same object as our  $\pi\eta$  enhancement since the missing-mass spectrometer was not able to establish the decay mode, although the results are consistent with a  $\pi\eta$  decay. If one uses only the data from the bubble-chamber experiments, one finds that the various results are not inconsistent with a resonance of width of about 50 MeV.

#### ACKNOWLEDGMENTS

We thank the operating crews of the ZGS and of the 30-in. bubble chamber for their cooperation and also our scanning and measuring staff for their careful work.

## Photoproduction of $K^+$ Mesons and Polarization of $\Lambda^0$ Hyperons in the 1-GeV Range\*

T. FUJII, A. IMANISHI, S. IWATA, A. KUSUMEGI, M. MISHINA, T. MIYACHI, H. SASAKI, AND K. TAKAMATSU  
*Institute for Nuclear Study, University of Tokyo, Tokyo, Japan*

AND

S. ORITO AND F. TAKASAKI  
*Department of Physics, University of Tokyo, Tokyo, Japan*

AND

M. HIGUCHI  
*Faculty of Engineering, Tohoku-Gakuin University, Miyagi, Japan*

AND

T. AMENO  
*Faculty of Engineering Science, Osaka University, Osaka, Japan*

AND

S. HOMMA  
*Department of Physics, Tohoku University, Sendai, Japan*  
(Received 23 June 1969; revised manuscript received 16 March 1970)

Polarization of  $\Lambda$  hyperons and differential cross sections for the reaction  $\gamma + p \rightarrow K^+ + \Lambda$  were measured at the  $K^+$ -meson center-of-mass angles around  $45^\circ$ ,  $70^\circ$ , and  $90^\circ$  for the incident photon energies of 1054, 1100, and 1160 MeV. The  $K^+$  mesons were detected with a magnetic spectrometer and a velocity-selection system based on the energy loss and the time of flight. The polarization of  $\Lambda$  was determined by measuring the up-down asymmetry of protons in the decay  $\Lambda \rightarrow p\pi^-$  with respect to the production plane. The results show a dominant  $\sin\theta_K^*$  dependence of the polarization at the region of the third resonance and are consistent with a contribution of the  $P_{11}$  resonance with a mass of about 1700 MeV.

### I. INTRODUCTION

RECENT developments in the phase-shift analysis<sup>1-5</sup> of the pion-nucleon elastic scattering have

\* Theses based on a part of this work have been submitted to the University of Tokyo by S. Orito and S. Iwata in partial fulfillment of the requirement for the degree of Doctor of Philosophy.

<sup>1</sup> L. D. Roper, R. M. Wright, and B. T. Feld, *Phys. Rev.* **138**, B190 (1965).

<sup>2</sup> P. Bareyre, C. Bricman, and G. Villet, *Phys. Rev.* **165**, 1730 (1968).

<sup>3</sup> A. Donnachie, R. G. Kirsopp, and C. Lovelace, *Phys. Letters* **26B**, 161 (1968).

<sup>4</sup> A. T. Davis and R. G. Moorhouse, in *Proceedings of the*

revealed the presence of many resonant states in the mass region below 2 GeV. In particular, at the region of the third resonance, where the well-established resonances  $D_{15}(1680)$  and  $F_{15}(1688)$  dominate, there exist several kinds of indications for the presence of resonances,  $S_{11}$  near 1710 MeV and  $P_{11}$  around 1750 MeV.<sup>2-5</sup> Independent evidence for the  $S_{11}$  and  $P_{11}$

*Fourteenth International Conference on High-Energy Physics, Vienna, 1968* (CERN, Geneva, 1968).

<sup>5</sup> C. Lovelace and F. Wagner, in *Proceedings of the Fourteenth International Conference on High-Energy Physics, Vienna, 1968* (CERN, Geneva, 1968).



radiator of  $1.7 \times 10^{-2}$  radiation length and defined, at a distance of 2.6 m from the radiator, by a lead collimator with an aperture of 5 mm in diameter. At a distance of 12.8 m from the radiator, the beam illuminated a target, containing liquid hydrogen in a cylindrical cup of Mylar, 14.8 cm in length and 6.0 cm in diameter. The axis of the Mylar cup was set along the center line of the beam within an accuracy of  $\pm 2.5$  mm. The total energy of the photon flux was continuously monitored by a thick-walled ionization chamber,<sup>16</sup> which was calibrated with a quantameter and a Faraday cup. The beam intensity during the experiment was typically  $1.5 \times 10^9$  equivalent quanta/sec. A typical beam spill was 4 msec centered at the top field of the synchrotron magnet.

#### A. Counter System

The detection system, shown in Fig. 1, consisted of a magnetic spectrometer for detecting  $K^+$  mesons on one side of the beam line and, on the other side, two identical counter telescopes above and below the production plane for detecting decay protons from  $\Lambda$  hyperons in coincidence with the  $K^+$  mesons.

The spectrometer magnet was of sector-shaped and horizontal-focusing type with a gap distance of 10 cm. For the central orbit, the bending angle was  $50^\circ$ , the radius of curvature 120 cm, the path length 6.2 m between a source and a focal point. The absolute momentum was calibrated with an accuracy of  $\pm 0.5\%$  by means of the floating-wire method.

The angular acceptance of the spectrometer was  $\pm 3.1^\circ$  horizontally and  $\pm 0.5^\circ$  vertically, which was defined by the counter  $S_2$  placed in front of the magnet. The vertical size of  $S_2$  was determined so that the particles produced at the target and being detected by this counter did not hit the pole face of the magnet. The momentum of the particles was defined by the counters  $K_H$  and  $K_L$  placed at the focal point. Each of them had a width of 11 cm, which corresponded to the momentum acceptance of  $\pm 2.3\%$ . The counter  $S_1$  in front of  $S_2$  was necessary not only to eliminate the background particles which fired  $S_2$  by producing the Čerenkov light in its Lucite light pipe, but also to reduce accidentals. The counter  $S_3$  and  $S_4$  rejected the unwanted particles scattered by the magnet yoke.

Two Čerenkov counters of total reflection type,  $\check{C}_1$  and  $\check{C}_2$ , were used to reject the copious background of  $\pi^+$  mesons. The Čerenkov radiator was a polished Lucite slab of 4.4 cm thickness with an area of  $25 \times 22$  cm<sup>2</sup>. Both sides of the radiator were tapered and coupled to the phototubes RCA-8575 with silicon grease. The radiator was contained in a box whose inner surface was covered with a black cloth of felt so that only light reflected at internal surfaces of the Lucite can reach the phototubes. The coincidence was required

<sup>16</sup> Y. Murata and S. Watanabe, Tokyo University Report No. INS-TH-53, 1966 (unpublished); T. Miyachi *et al.* (private communication).

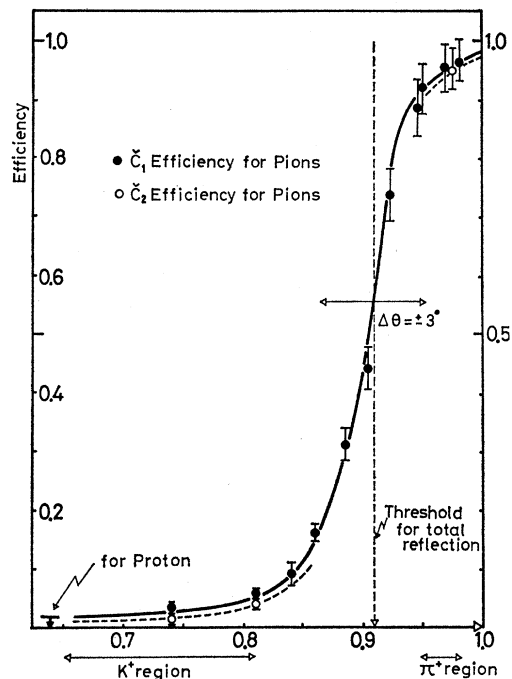


FIG. 2. Velocity dependence of Čerenkov-counter efficiency at the bias setting in the data-taking runs. The velocity range indicated by  $\Delta\theta$  shows the variation of the threshold velocity in the angular divergence of  $\pm 3^\circ$ .

between the pulses from the left and right phototubes in order to reduce the unwanted signals associated with the  $K^+$  mesons caused by the scatterings, by the  $\delta$  rays, and by the irregular reflections of the light. The threshold velocity of the counter is  $0.91c$ , corresponding to the critical angle for the total reflection in the Lucite. Over the momentum range of this experiment, i.e., 415–685 MeV/c, the range of the velocity was  $0.95$ – $0.98c$  for the pions, and  $0.65$ – $0.81c$  for the  $K^+$  mesons. The velocity dependence of the efficiencies of  $C_1$  and  $C_2$ , shown in Fig. 2, was measured with the  $\pi^-$  mesons detected by the spectrometer based on the pulse height and time of flight. Each of the counters detected about 96% of the highly relativistic  $\pi^-$  mesons. Though the present velocity range of the  $K^+$  mesons was well below the threshold, the Čerenkov counters responded to about 2% of pions which simulated the  $K^+$  mesons at the momentum range of the present experiment.

The counter  $E$  placed at the end of the spectrometer was designed for the measurement of specific ionization. The counter was made of a plastic scintillator of 2 cm thickness with an area of  $24 \times 22$  cm<sup>2</sup>, which was viewed from both sides by 56 AVP through Lucite light guides. An aluminum foil was used as a reflector which was separated from the scintillator by 1 cm. This structure served to improve the local pulse-height uniformity of the counter. By adding the pulses from the phototubes at both sides, a pulse-height variation smaller than 4% was obtained over all the area. A final resolution of this

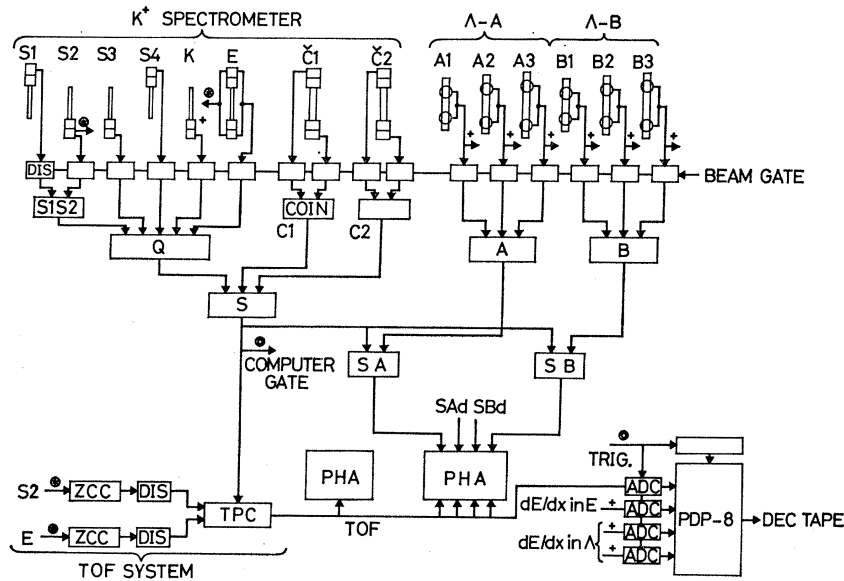


FIG. 3. Block diagram of logic system. ZCC is a fast zero-crossing circuit.

counter was  $\pm 14\%$  for the minimum-ionizing particles accepted by the spectrometer. The greatest part of the resolution was due to the intrinsic Landau fluctuation of the specific ionization loss.

The time of flight of the particles was measured between the counters  $S_2$  and  $E$ . The flight path was 4.5 m, which corresponded to a time difference of 3.1 nsec between the pion and the  $K^+$  meson at the maximum momentum setting of 685 MeV/c. The block diagram of the time-of-flight system is shown in a part of Fig. 3. In order to reduce the time walk associated with the pulse-height fluctuation, clipped pulses from the two counters were sent to fast zero-crossing circuits whose time walks were less than 0.6 nsec in the dynamic range of the pulse-height variation of 30. The overlapping time between the timing signals was then measured by a time-to-pulse-height converter (Chronetics Model 105). A further improvement of the time resolution was made by canceling the path difference through the magnet. Between the two extreme orbits through the magnet, there exists the maximum path difference of 30 cm, which corresponds to a time difference of 1.4 nsec for a particle with a velocity of  $\beta=0.7$ . The effect of this path difference was successfully eliminated by viewing the scintillator of  $S_2$  from the side close to the shorter orbit. In this case, the path difference was compensated by the transit-time difference, which was about 1 nsec, of the light in the scintillator of  $S_2$ . In addition, the time of arrival at the  $E$  counter was determined within  $\pm 0.2$  nsec, independently on the beam position. In this way, the time resolution of  $\pm 0.7$  nsec was achieved.

Two identical telescopes placed above and below the production plane detected the decay protons from  $\Lambda$ . Each telescope consisted of three scintillation counters  $A_1, A_2, A_3$  (or  $B_1, B_2, B_3$ ). The front counter  $A_1$  ( $B_1$ ) was the defining counter with a solid angle of about 41

msr and the others were oversized. The six counters were mounted on a table, the three counters up and the others down, so that the two telescopes could be easily interchanged. In the interchanging, the vertical positions of the up and the down telescopes were reproduced with an accuracy of  $\pm 0.2$  mm. Each of the six counters was viewed by two 56 AVP through Lucite light guides in a vertical direction. By adding the pulses from the two phototubes, a pulse-height resolution of  $\pm 30\%$  was obtained for the minimum-ionizing particles.

### B. Logic System

The block diagram of the logic system is shown in Fig. 3. The passage of a particle through the spectrometer was defined by a fast-coincidence logic:

$$Q = (S_1 \cdot S_2) \cdot S_3 \cdot S_4 (K_H \text{ or } K_L) \cdot E.$$

The copious background of a thousand times as many pions as the  $K^+$  mesons was reduced to a comparable number of the  $K^+$  mesons by a pair of Čerenkov counters put in anticoincidence with the logic  $Q$ :

$$S = Q \cdot \bar{C}_1 \cdot \bar{C}_2,$$

which was a master coincidence signal with a resolving time of 25 nsec. On the other side, threefold coincidences

$$A = A_1 \cdot A_2 \cdot A_3 \quad \text{and} \quad B = B_1 \cdot B_2 \cdot B_3$$

for two  $\Lambda$  telescopes were signals of the passage of particles in the direction of decay protons. A two-arm coincidence for the selection of the  $\Lambda$ -decay protons was made with 20-nsec time resolution between the master coincidence  $S$  and the  $\Lambda$  logics:

$$SA = S \cdot A \quad \text{and} \quad SB = S \cdot B.$$

Accidental coincidence rates were continuously monitored with logics containing suitably delayed signals.

The data were recorded into scalars, a pulse-height analyzer (TMC 404), and an on-line data storage system. The 400-channel memory of the pulse-height analyzer was divided into four segments, which stored the time-of-flight spectra gated separately by the two-arm coincidence signals,  $SA$ ,  $SB$  and the corresponding accidental signals. At each occurrence of the event satisfying the master coincidence  $S$ , the on-line data storage system stored the eight-word information into the memory of a PDP-8 computer, including a magnet current, the presence of ten kinds of fast logic signals, the time of flight, and three kinds of pulse heights, in addition to labels consisting of run number, target full or empty, and name of up  $\Lambda$  telescope. The stored data were summarized and printed out in a desired form at each run. After accumulating 208 events, the stored raw data were transferred to a DEC microtape. They were analyzed off line to obtain final  $K^+$  yields and other useful information.

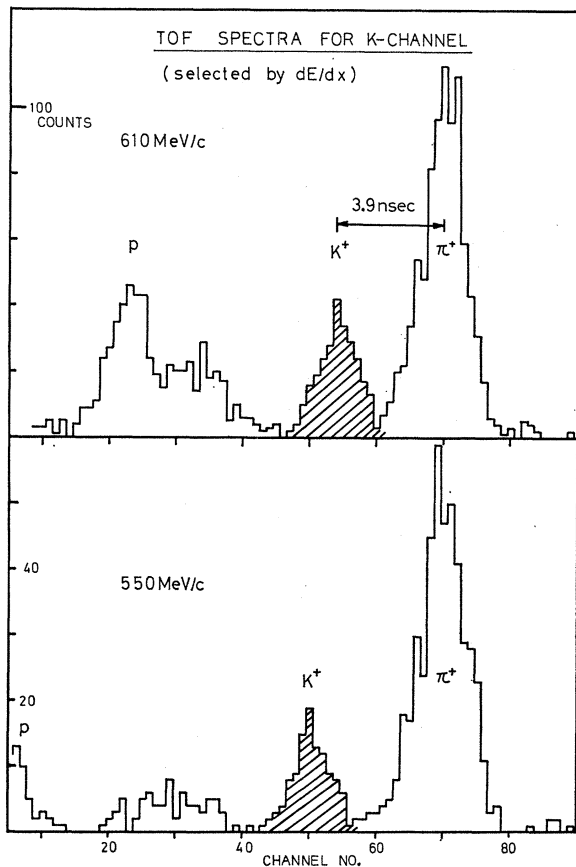


FIG. 4. Typical time-of-flight (TOF) spectra for the events satisfying the master coincidence  $S$ . The pulse height in the last counter was selected by a computer program.

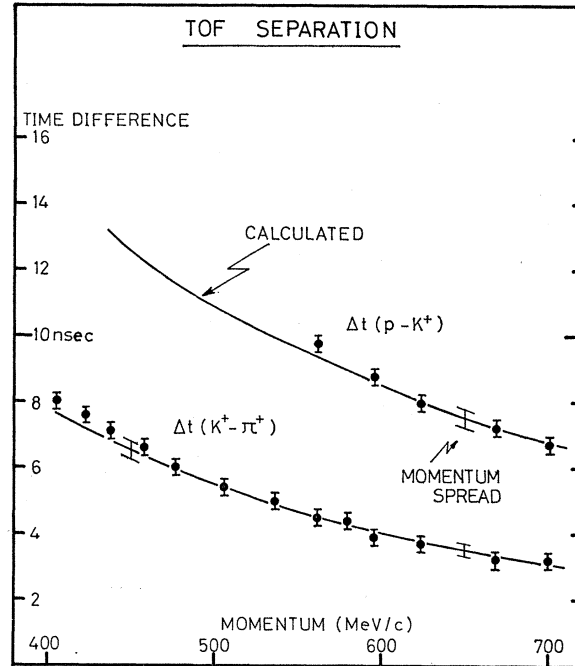


FIG. 5. Time-of-flight separation among protons,  $K^+$  mesons, and pions.

### III. EXPERIMENTAL PROCEDURE

#### A. Identification of Reaction

Typical examples of the time-of-flight spectra recorded into the microtapes are shown in Fig. 4. As seen in this figure, a clear peak was observed in each spectrum at the position expected for the  $K^+$  mesons. The peak was proved to be due to the  $K^+$  mesons in the following procedures.

(i) The time-of-flight spectrum was measured for the various momentum settings. As presented in Fig. 5, the time differences among the observed peaks agree well with the differences expected for the pions, the  $K^+$  mesons, and the protons.

(ii) The correlation between the time of flight and the pulse height was investigated by the off-line analysis of the magnetic tape information. Figure 6 shows an example of the two-dimensional plot. In each of the plots obtained, three groups of the points were clearly observed, whose pulse height and time of flight were in good agreements with the expected ones for the pions, the  $K^+$  mesons, and the protons.

(iii) Fixing the momentum and the angle of the spectrometer, the maximum photon energy of the beam was lowered. The peak of the  $K^+$  meson disappeared at the energy below the threshold for the production of the  $K^+$  meson, whereas the peaks of the pion and the proton remained. The over-all behavior of the  $K^+$ -photoproduction reaction was checked by the excitation curve measured at  $19.3^\circ$  and  $557 \text{ MeV}/c$ . The two rises

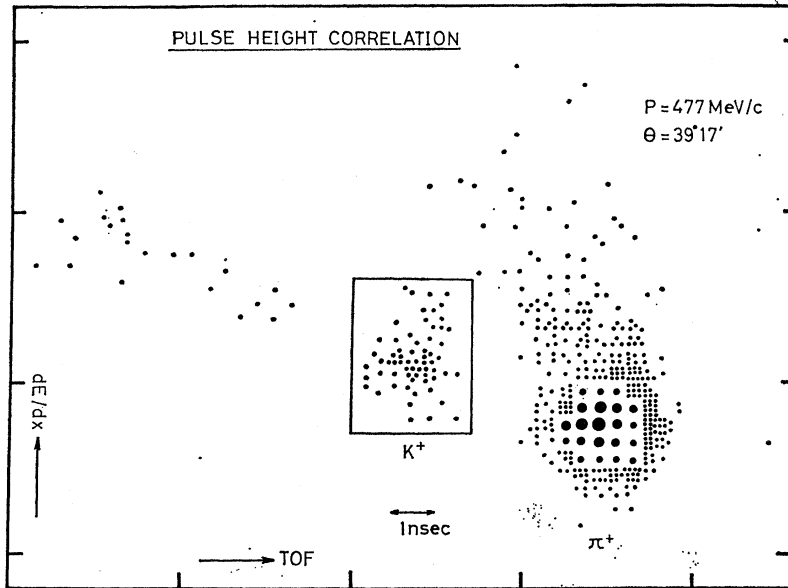


FIG. 6. Pulse-height correlation between the time of flight and the energy loss. Most of the protons were eliminated by coincidence timing for this momentum.

at the thresholds of the  $\Lambda$  and the  $\Sigma^0$  productions and a flat region between them were found as expected.

Typical time-of-flight spectra obtained for the two-arm coincidence are shown in Fig. 7, where the pulse-height selection for the counter  $E$  has been made with a computer program. As is evident from the figure, the subtraction of the accidentals leaves a single-peak spectrum, in which the location of the peak coincides with that of the  $K^+$  mesons qualified by the previous time-scale calibration. This fact indicates a clean detection of the decay protons from the  $\Lambda$  hyperons which were associated with the  $K^+$  mesons. The events with the time of flight at the  $K^+$  region were identified as the desired ones. A further proof for the detection of the decay protons comes from the measurements of the pulse heights in the  $\Lambda$  counters. During the data-taking runs, the pulse heights in two of the  $\Lambda$  counters were recorded on the magnetic tape for each two-arm coincidence. Figure 8 gives a typical two-dimensional plot of the pulse heights in  $A_2$  and  $A_3$ . As is expected, the events identified as the decay protons give the correlated pulse heights which are much larger than that of the relativistic particles.

### B. Measurement of Polarization

The angular distribution of the decay protons in the rest frame of  $\Lambda^0$  is given by

$$N(\phi)d\Omega = (4\pi)^{-1}(1 + \alpha P_\Lambda \cos\phi)d\Omega,$$

where the asymmetry parameter  $\alpha$  has the value of  $+0.646 \pm 0.016$ ,<sup>17</sup>  $P_\Lambda$  is the polarization of the  $\Lambda^0$ , and

<sup>17</sup> A. H. Rosenfeld *et al.*, Rev. Mod. Phys. **41**, 109 (1969).

$\phi$  is the angle between the direction of the polarization and the direction of motion of the decay protons. The up-down asymmetry  $R$  is related to the polarization  $P_\Lambda$

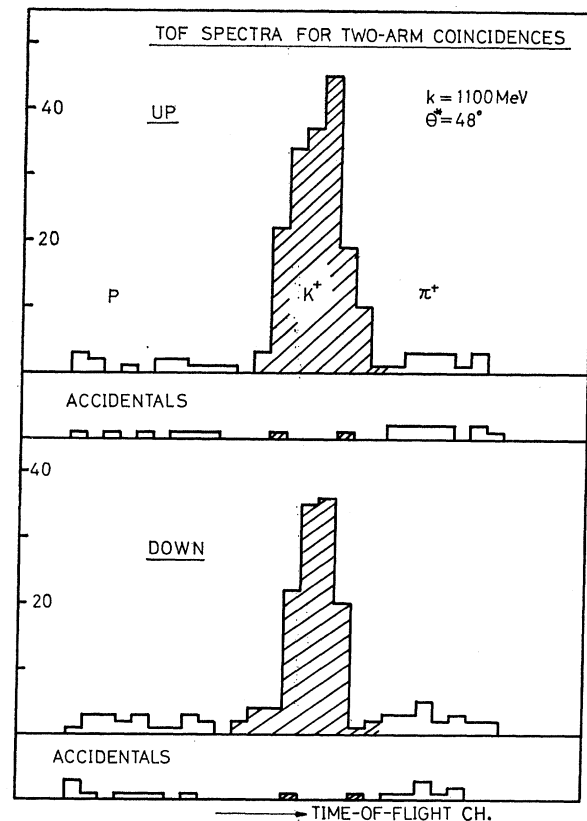


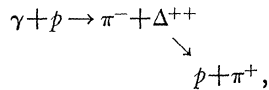
FIG. 7. Time-of-flight spectra for the events satisfying the two-arm coincidences.

in the direction  $\mathbf{k}_\gamma \times \mathbf{p}_\Lambda$  by

$$R \equiv \frac{N_u - N_d}{N_u + N_d} = \alpha P_\Lambda \langle \cos\phi \rangle,$$

where  $N_u$  and  $N_d$  are the counting rates of the telescopes above and below the production plane, respectively, and  $\langle \cos\phi \rangle$  is the average value of  $|\cos\phi|$  for protons detected by the telescopes. The value of  $\langle \cos\phi \rangle$  was computed by a Monte Carlo method with an accuracy of  $\pm 2\%$ , taking into account the acceptances of the spectrometer and the telescopes, and the size of interaction volume.

In order to minimize the systematic asymmetry, the following procedures were repeated in the asymmetry measurement. The  $x$ -ray films were exposed and photometrically analyzed to monitor the position and the direction of the incident beam at each energy. The detector misalignment relative to the production plane was found to be of the order of 1 mrad. The telescopes were regularly interchanged, up for down, by rotating around the symmetric axis to eliminate a small difference in the detection efficiency for decay protons. Furthermore, as a check for unpolarized samples, we used the reaction



where the spectrometer detected the  $\pi^-$  meson and the telescopes detected the decay protons from  $\Delta^{++}$ . Because of the proximity of kinematical parameters between the  $\pi^- \Delta^{++}$  and the  $K^+ \Lambda$  reactions, check runs were made without changing the detector geometry

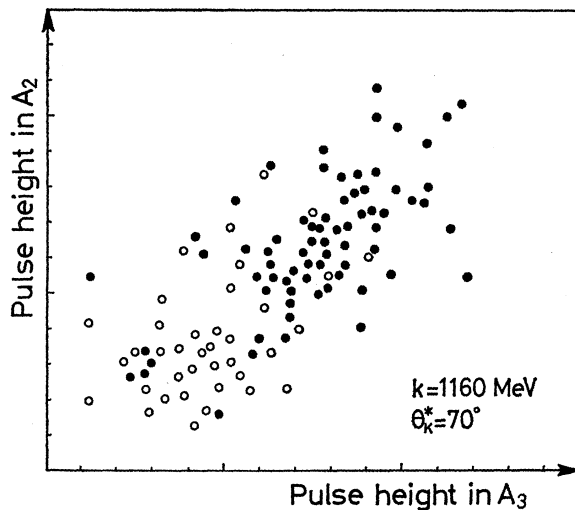


FIG. 8. Pulse-height correlation in A counters. Closed circles represent the events identified as decay protons. Open circles correspond to the relativistic particles. Six closed circles at a region of the minimum ionization are due to the accidental two-arm coincidences.

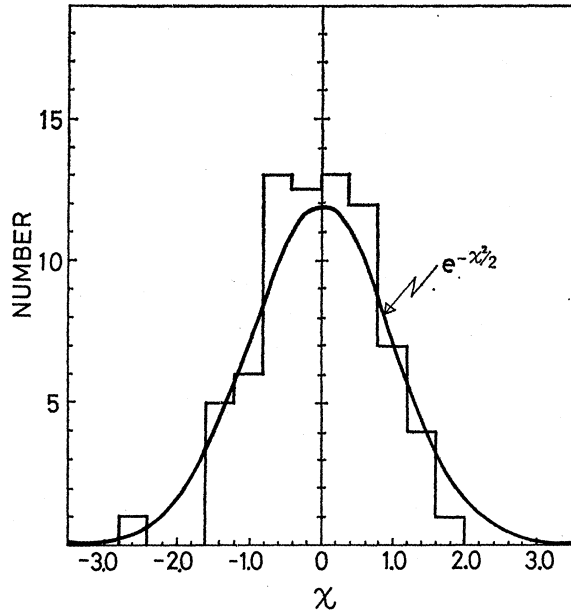


FIG. 9. Run-by-run fluctuation of the polarization measurement.

in each setting. The asymmetry for the unpolarized sample was found to be consistent with zero within a statistical error of  $\pm 0.04$ . This assured us that the systematic error was much smaller than the statistical one in our measurement.

The data were taken by setting the maximum photon energy to 70 MeV above the responsible photon energy. It was possible by this setting to eliminate the contamination from the reaction  $\gamma p \rightarrow K^+ \Sigma^0$  without losing the desired event.

Typically 500 decay protons were detected at each kinematical point. The measurement at a point was divided into about ten short runs. The asymmetry  $R$  at the kinematical point was defined as the weighted mean of  $R_i$ , where  $R_i$  is the asymmetry of the  $i$ th run. Consistency among the runs was checked by monitoring the run dependence of the measured asymmetry; however, no indications for the systematic run dependence was observed throughout the experiment. The quantity  $\chi$  was calculated for each run by

$$\chi_i = (R - R_i) / \Delta R_i.$$

The obtained  $\chi$  distribution for all the runs is given in Fig. 9. The distribution agrees well with the Gaussian form which is statistically expected.

### C. Reduction of Differential Cross Sections

For the determination of absolute  $K^+$  yields, the computer stored all the events that satisfied the master coincidence  $S$ . The  $K^+$  yields were obtained easily from the two-dimensional plots, as shown in Fig. 6, with the uncertainty less than 4%. The  $K^+$  data were taken at 18 kinematical points with a center-of-mass angular

TABLE I. Systematic error of the cross section.

Spectrometer aperture	$\pm 3.0\%$
Momentum setting	$\pm 0.7\%$
Čerenkov efficiency	$\pm 2.0\%$
Decay correction	$\pm 2.0\%$
Absorption correction	$\pm 4.0\%$
Multiple scattering	$\pm 0.5\%$
Target constants	$\pm 1.0\%$
$K^+$ selection	$\pm 4.0\%$
Beam monitor	$\pm 3.0\%$
Bremsstrahlung shape factor	$\pm 1.0\%$
Electronic efficiency	$\pm 2.0\%$
Total rms uncertainty	$\pm 9\%$

resolution ranging from  $\pm 5.0^\circ$  to  $\pm 6.5^\circ$  and with a laboratory photon energy resolution from  $\pm 1.1$  to  $\pm 2.9\%$ . The spectrometer was always set to a momentum corrected for the average energy loss of  $K^+$  mesons in materials before the magnet. The  $K^+\Lambda$  reaction was observed with a bremsstrahlung whose end-point energy was typically lower by 1% than the lowest photon energy responsible to the  $K^+\Sigma^0$  reaction. The counting statistics required from the polarization measurement gave sufficient  $K^+$  yields owing to the detection efficiency of 20% for the  $\Lambda$ -decay protons in the  $\Lambda$  telescopes. In addition to the  $K^+\Lambda$  data, the  $K^+\Sigma^0$  reaction was observed at two angles for a laboratory photon energy of 1180 MeV. In this case, the  $K^+\Sigma^0$  yield was obtained by subtracting the contributing  $K^+\Lambda$  yield.

Background runs were made with an empty hydrogen cup. The counting rate of those background events qualified for the  $K^+$  mesons was observed to vary from 7 to 10%. It was in good agreement with a value calculated with the data on the  $K^+\Lambda$  photoproduction in nuclei.<sup>18</sup> As a result, the measured background counts were directly subtracted from the  $K^+$  yield obtained with a full target.

Although the typical counting rate of accidental coincidence in the master logic  $S$  changed from 2 to 4%, the selected  $K^+$  yields contained negligible amounts of them since the accidentals were predominantly caused by protons or pions which were identified in the course of the off-line analysis. The information from scalers was used to correct the observed counts for the dead time of the data storage system.

The net yield  $Y$  of  $K^+$  mesons and the differential cross section averaged over the system acceptance are related as follows:

$$Y = BHC\eta \langle d\sigma/d\Omega \rangle,$$

where  $C$  and  $B$  are the product of kinematical factors and the total flux of photons, respectively.  $H$  describes constants characterizing the target and spectrometer system, while  $\eta$  is the detection efficiency. The absolute calibration constant of the thick-walled ionization chamber is now known with uncertainty less than 3%,

<sup>18</sup> A. J. Sadoff and B. D. McDaniel, Phys. Rev. **133**, B1200 (1964).

while its relative error among different end-point energies of the bremsstrahlung is better than 0.5%. The spectrometer aperture was calculated with a linear approximation obtained from a floating-wire method and field measurement. The effects of the finite target size and of the beam profile were taken into account. A typical value was found to be  $1.03 \times 10^{-4}$  sr, whose error due to the nonlinear effect was estimated to be 2%. The error arising from the misalignment of the system was calculated with a displaced beam intensity distribution, resulting in 0.4% difference.

The detection efficiency consists of various factors as described below. The electronic counting loss was less than 3%, mainly due to the dead time of discriminators for the front counters. The finite detection efficiency of a pair of Čerenkov counters below the threshold velocity caused a counting loss of  $K^+$  mesons of from 3 to 10% which was determined by the calibration simulated by pions. The uncertainty of 2% was assigned to this on the basis of the finite efficiency below the emission threshold for the Čerenkov light and the counting statistics in the calibration runs. The counting loss of a rear aperture counter due to the multiple Coulomb scattering was calculated to be less than  $(2.0 \pm 0.5)\%$  even in the presence of the front absorber.

Because of the short lifetime, 70–87% of the  $K^+$  mesons decayed in passing through the telescope. Because most of the relativistic decay products were rejected by the time-of-flight selection and the Čerenkov counters placed in front of the rear aperture, the contribution of the decay products to the observed  $K^+$  yields required a minor correction. The correction

TABLE II. Experimental results.  $k_\gamma$  is the mean  $\gamma$ -ray energy in MeV.  $\theta_K$  is the center-of-mass angle for the  $K^+$  meson in degrees.

(a) Polarization			(b) Differential cross section		
$k_\gamma$	$\theta_K$	$P_\Lambda$	$k_\gamma$	$\theta_K$	$\frac{d\sigma}{d\Omega}$ ( $10^{-31}$ cm <sup>2</sup> /sr)
1160	46.0	$0.54 \pm 0.09$			$\gamma + p \rightarrow K^+ + \Lambda^0$
1160	70.0	$0.44 \pm 0.10$			
1160	90.0	$0.27 \pm 0.14$	1170	46.0	$2.47 \pm 0.15$
1100	47.6	$0.38 \pm 0.12$	1175	69.5	$1.96 \pm 0.12$
1100	72.8	$0.48 \pm 0.10$	1172	89.0	$1.35 \pm 0.12$
1100	94.4	$0.32 \pm 0.19$	1150	46.5	$2.53 \pm 0.09$
1054	49.8	$0.28 \pm 0.12$	1150	71.0	$2.09 \pm 0.11$
1054	76.8	$0.07 \pm 0.13$	1150	91.0	$1.31 \pm 0.14$
			1113	47.5	$2.34 \pm 0.12$
			1110	72.5	$2.04 \pm 0.13$
			1110	93.5	$1.41 \pm 0.08$
			1090	48.0	$2.48 \pm 0.12$
			1090	73.5	$2.09 \pm 0.10$
			1090	96.0	$1.32 \pm 0.08$
			1064	49.0	$2.59 \pm 0.17$
			1064	76.0	$1.87 \pm 0.09$
			1047	50.5	$2.37 \pm 0.15$
			1047	78.0	$1.72 \pm 0.11$
			1005	54.0	$1.41 \pm 0.13$
			994	56.5	$1.12 \pm 0.12$
					$\gamma + p \rightarrow K^+ + \Sigma^0$
			1180	54.0	$1.54 \pm 0.36$
			1180	84.0	$1.23 \pm 0.28$

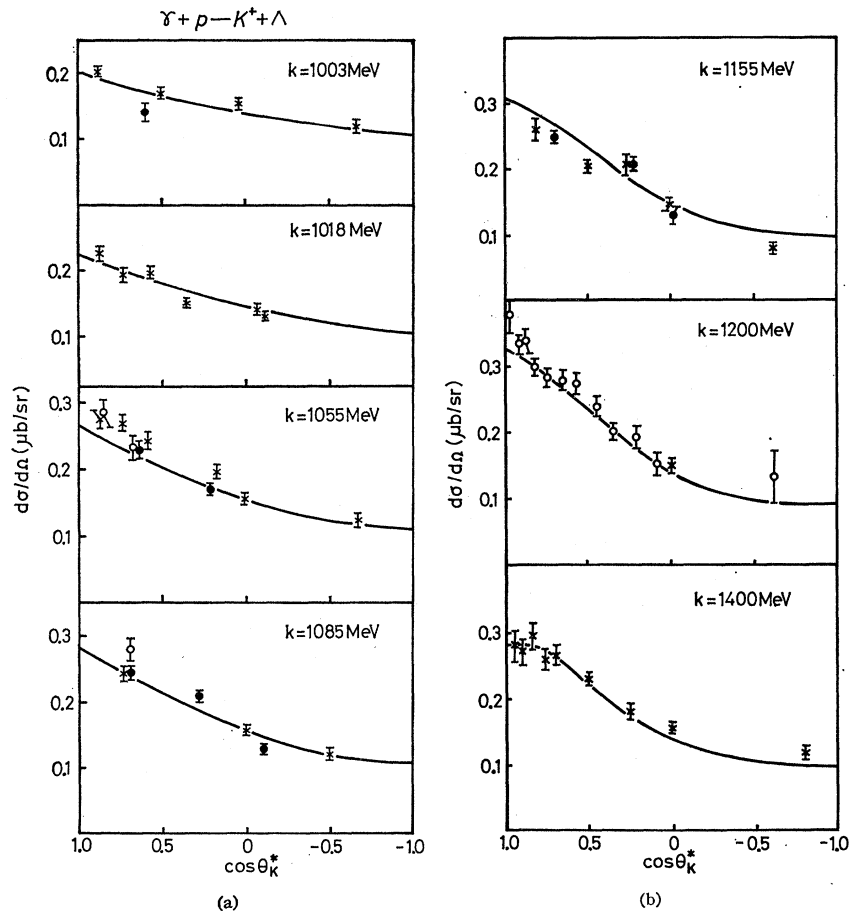


FIG. 10. Differential cross sections for the reaction  $\gamma + p \rightarrow K^+ + \Lambda$ . The solid curve is a fit obtained by the partial-wave analysis as explained in the text. The data symbols used in the figure are the same as in Fig. 11. The present data points are represented by the closed circles.

was calculated assuming a uniform  $K^+$  beam after the magnet, taking into account the dominant two-body decay. The particles from the backward decay after the aperture contributed negligibly. A small amount of the forward decay products was found to be contained in the observed  $K^+$  yield, ranging from 1.5% at 700 MeV/c to 0.8% at 400 MeV/c. The loss of  $K^+$  mesons caused by the nuclear interaction was calculated by means of a simple optical model<sup>19</sup> from which total absorption cross sections were obtained. The momentum dependence of the cross section<sup>20</sup> was safely ignored in the momentum range between 420 and 700 MeV/c. The calculation yielded an absorption loss of 9.0% in the presence of a polyethylene absorber and 8.3% otherwise, with an uncertainty of 4% including the large error of the absolute nuclear cross sections.

Those uncertainties that contribute equally to all the data points and that change slowly with experimental settings are treated as systematic errors, which are summarized in Table I. The combined systematic error in the absolute cross sections comes out to be 9%.

<sup>19</sup> S. Fernbach, R. Serber, and T. B. Taylor, Phys. Rev. **75**, 1352 (1949).

<sup>20</sup> B. S. Zorn and G. T. Zorn, Phys. Rev. **120**, 1898 (1960); S. Goldhaber *et al.*, Phys. Rev. Letters **9**, 135 (1962).

#### IV. RESULTS AND DISCUSSION

The results of the polarization measurement are summarized in Table II(a). The errors attached to the polarization are statistical only and do not include the following uncertainties: (a) errors in  $\alpha_\Lambda$  ( $0.646 \pm 0.016$ ), (b) an uncertainty of  $\pm 2\%$  in calculating the  $\langle \cos \phi \rangle$  by means of the Monte Carlo method, (c) the error of the asymmetry of about  $\pm 0.02$  arising from the uncertainty of  $\pm 1$  mrad in the relative position of the  $\Lambda$  telescopes to the production plane. These uncertainties lead to a possible systematic error of about  $\pm 0.04$  for the  $\Lambda$  polarization, in contrast to a typical statistical error of  $\pm 0.12$ .

In addition, we have also obtained 18 values of differential cross sections for  $\gamma + p \rightarrow K^+ + \Lambda^0$  as well as those for  $\gamma + p \rightarrow K^+ + \Sigma^0$  at two kinematical settings. The results are tabulated in Table II(b), where quoted errors are statistical, including a contribution from the background subtraction. Most of them are in good agreement with the previous measurements performed in this energy range as shown in Figs. 10(a) and 10(b).

Results on the polarization are shown in Fig. 11 as a function of the c.m. angle. As seen in this figure, the present measurements near  $90^\circ$  are in good agreement

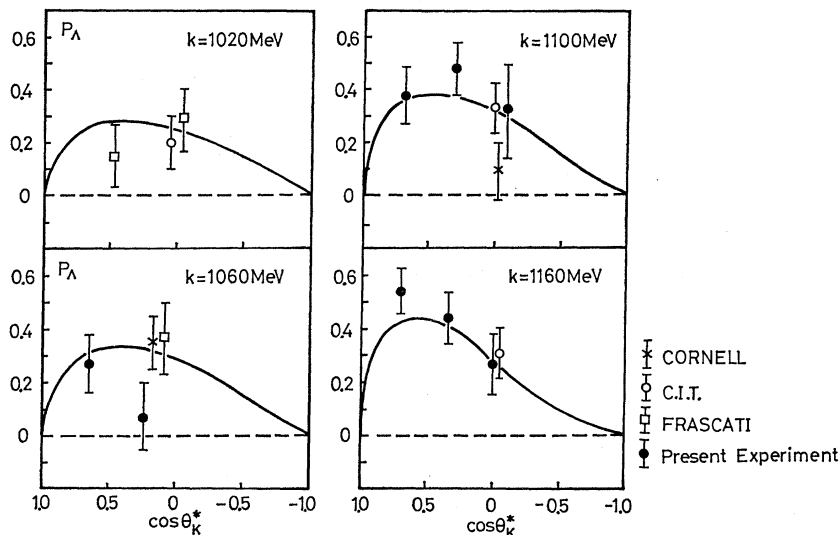


FIG. 11. Angular dependence of the  $\Lambda$  polarization. The solid curve is a fit obtained by the partial-wave analysis.

with the existing data. However, our measurement at  $\theta_{K^*} = 77^\circ$  and  $k = 1054$  MeV is smaller than the previous measurements at Cornell at  $\theta_{K^*} = 80^\circ$  and of Frascati at  $85^\circ$  by about 2 standard deviations. Checks were repeated at this point for the systematic errors, but no possible source of error was found except for a statistical fluctuation.

The present measurements have revealed the dominant  $\sin\theta_{K^*}$  dependence of the  $\Lambda$  polarization at the region of the third resonance. This angular dependence of the polarization clearly indicates the insignificance of high-wave resonances such as  $D_{15}(1680)$  or  $F_{15}(1688)$  and may suggest a contribution of the resonance with a low angular momentum. In addition, the differential cross sections require terms up to quadratic when expanded in a power series of  $\cos\theta^*$ . The presence of a  $P$  wave shows up in the  $S$ - $P$  interference term which contributes strongly above 1000 MeV. However, a simple resonance picture cannot be applied to the cross-section data since the interference term does not change the sign. For further quantitative discussions on this point, a multipole analysis<sup>21</sup> of the reaction was carried out using our new data as well as the existing ones. In the analysis, the background amplitudes were assumed to have a smooth energy dependence, and resonances are considered in  $S_{11}$ ,  $P_{11}$ , and  $D_{13}$  states besides the well-established resonances  $D_{13}(1518)$ ,  $D_{15}(1680)$ , and  $F_{15}(1688)$ . Solution were obtained which fitted the data well. The fit by a typical solution is shown in Figs. 10 and 11 by solid lines.

<sup>21</sup> S. Orito, Ph.D. thesis, Tokyo University Report No. INS-J-113, 1969 (unpublished); S. Iwata, Ph.D. thesis, Tokyo University Report No. INS-J-115, 1969 (unpublished).

In these solutions, the main features of the polarization data are accounted for by the interference between a  $P_{11}$  resonance ( $M \sim 1700$  MeV,  $\Gamma \sim 210$  MeV) and the dominant  $S$ -wave background. Without the  $P_{11}$  resonance, it was difficult to fit the energy and angular dependences of the  $\Lambda$  polarization. The contribution from the well-known high-angular-momentum states such as  $D_{13}(1518)$ ,  $D_{15}(1680)$ , and  $F_{15}(1688)$  were found to be insignificant, as might be expected directly from the observed angular dependence of the  $\Lambda^0$  polarization. On the other hand, a steep forward rise of the polarization at  $k = 1160$  MeV suggests a rapid growth of the imaginary amplitude of  $P_{13}$  and/or  $D_{13}$  waves with increasing energy. Further measurements on the polarization at higher energies and backward angles are needed to see if this is due to the effect of higher resonances. No indication is observed for the resonance  $S_{11}(1710)$  in contrast to its dominance in the reaction  $\pi^- + p \rightarrow K^0 + \Lambda$ . It is interesting to note that the transition  $\gamma p \rightarrow S_{11}(1710)$  is forbidden according to a quark-model assignment of baryon resonance.<sup>22</sup>

#### ACKNOWLEDGMENTS

We would like to thank the operating staff of the Institute for Nuclear Study Electron Synchrotron under the direction of Professor S. Yamaguchi for their continuous cooperation throughout the experiment. Special thanks are due to K. Watanabe, M. Kasuya, Y. Akino, Y. Doi, and T. Kitami for their technical assistance.

<sup>22</sup> R. G. Moorhouse, Phys. Rev. Letters 16, 772 (1966).